

AN EXPLICIT SOLUTION TO THE OPTIMAL LQG PROBLEM FOR FLEXIBLE STRUCTURES WITH COLLOCATED RATE SENSORS*

A. V. Balakrishnan

Electrical Engineering Department
UCLA
Los Angeles, California

ABSTRACT

We present a class of compensators in explicit form (not requiring numerical computer calculations) for stabilizing flexible structures with collocated rate sensors. They are based on the explicit solution, valid for both Continuum and FEM Models, of the LQG problem for minimizing mean square rate. They are robust with respect to system stability (will not destabilize modes even with mismatch of parameters), can be instrumented in state space form suitable for digital controllers, and can be specified directly from the structure modes and mode "signature" (displacement vectors at sensor locations). Some simulation results are presented for the NASA LaRC Phase-Zero Evolutionary Model — a modal Truth model with 86 modes — showing damping ratios attainable as a function of compensator design parameters and complexity.

1. INTRODUCTION

In this paper we present a class of compensators for stabilizing flexible structures with collocated rate sensors for Continuum as well as Finite Element or truncated Modal models. They are derived by solving explicitly the optimal control corresponding to an LQG problem. The Compensator Transfer Functions are strictly positive real and as a result they are robust with respect to system stability. They can be determined based solely on the mode frequencies and mode "signatures" (displacements at the sensor sites) and can be instrumented directly in "state-space" form.

We begin in Section 2 with the LQG problem and its solution. Section 3 highlights the features of the Compensator Transfer Function. Section 4 is devoted to Continuum models where the transfer function is nonrational. The main result on controller design is in Section 5 which shows how to design the compensator from a modal model of the structure, and in particular, how to construct a hierarchy of compensators of increasing order. Simulation results, confined to stability properties (damping ratios), are by no means exhaustive and are presented in Section 6 based on the modal model of the NASA LaRC CSI Phase-Zero Evolutionary Model [4][†]. Noise response performance is not included but is expected to be good because of the LQG criterion optimization. Conclusions are in Section 7.

* Research supported in part under NAS-1-19158, NASA LaRC.

[†] References 1-6 are cited in text.

For recent related work on controller design for collocated sensors see [5, 6] and the references therein.

2. THE LQG PROBLEM AND ITS SOLUTION

To state the LQG problem, we begin with the canonical time-domain dynamics of a flexible structure with collocated rate sensors which, whether it is a Finite Element Model (and hence finite dimensional) or Continuum Model (and hence infinite-dimensional) can be expressed in the form:

$$\left. \begin{aligned} M\ddot{x}(t) + Ax(t) + Bu(t) + BN_a(t) &= 0 \\ v(t) &= B^*\dot{x}(t) + N_r(t) \end{aligned} \right\} \quad (2.1)$$

where in the case of FEM,

- M is the mass matrix (nonsingular, nonnegative definite)
- A is the stiffness matrix (nonsingular, nonnegative definite)
- B is the control matrix (rectangular matrix)
- $u(\cdot)$ is the control vector ($n \times 1$, assuming n actuators)
- $x(\cdot)$ is the “displacement” vector
- $N_a(\cdot)$ is the actuator noise assumed white Gaussian with spectral density $d_a I$, I being the $n \times n$ Identity matrix
- $v(\cdot)$ is the sensor output
- B^* represents the transpose of B
- $N_r(\cdot)$ is the sensor noise assumed white Gaussian with spectral density $d_r I$.

For the Continuum Model such a representation is still possible with $x(\cdot)$ now allowed to range in a Hilbert space (however complicated the structure), with A , M , and B being linear operators:

- M bounded linear, self-adjoint, nonnegative definite with M^{-1} bounded;
- A closed linear, self-adjoint, nonnegative definite with compact resolvent, resolvent, the resolvent set including zero
- B maps E^n Euclidean n -space into \mathcal{H} , and
- B^* represents the adjoint.

See [1], [2].

The LQG problem we shall consider is that of finding the control $u(\cdot)$ (or compensator) that minimizes the mean square time average:

$$\lim_{T \rightarrow \infty} \left\{ \frac{1}{T} \int_0^T \|B^* \dot{x}(t)\|^2 dt + \frac{\lambda}{T} \int_0^T \|u(t)\|^2 dt \right\} \quad (2.2)$$

where $\lambda > 0$. The optimal compensator transfer function ($n \times n$ matrix function) can be given in explicit form (see [1]):

$$\psi(p) = gpB^*(p^2M + A + \gamma pBB^*)^{-1}B, \quad \text{Re. } p > 0 \quad (2.3)$$

where

$$g = \frac{\sqrt{d_a/d_r}}{\sqrt{\lambda}}; \quad \gamma = \sqrt{d_a/d_r} + \frac{1}{\sqrt{\lambda}} \quad (2.4)$$

under the assumption that

$$B^*\phi_k \neq 0 \quad (2.5)$$

for any k , where ϕ_k are the modes orthonormalized with respect to the mass matrix:

$$A\phi_k = \omega_k^2\phi_k; \quad [M\phi_k, \phi_k] = 1. \quad (2.6)$$

In the finite-dimensional (e.g., FEM) case, the compensator can be realized in the (finite-dimensional) state space form:

$$u(t) = gB^*\dot{Y}(t) \quad (2.7)$$

$$M\ddot{Y}(t) + AY(t) + \gamma BB^*\dot{Y}(t) = Bv(t). \quad (2.8)$$

The corresponding mean square control power:

$$\lim_{T \rightarrow \infty} \frac{1}{T} \int_0^T \|u(t)\|^2 dt = \frac{d_a}{2\sqrt{\lambda}} \text{Tr. } (B^*MB)^{-1}. \quad (2.9)$$

The corresponding mean square displacement:

$$\lim_{T \rightarrow \infty} \frac{1}{T} \int_0^T \|B^*x(t)\|^2 dt = \left(\sqrt{d_a/d_r} + \frac{\sqrt{\lambda} d_a}{2} \right) \text{Tr. } B^*A^{-1}B. \quad (2.10)$$

Formulas (2.9) and (2.10) hold as well in the infinite-dimensional (Continuum Model) case.

3. FEATURES OF THE COMPENSATOR TRANSFER FUNCTION

Some significant features of the compensator transfer function which are noteworthy are:

(i) As $\lambda \rightarrow 0$, $\psi(p) \rightarrow I\sqrt{d_a/d_r}$ we note that

$$\psi(p) = I\sqrt{d_a/d_r}$$

is the optimal "static" or "direct connection" or "PID" controller. Note that as $\lambda \rightarrow 0$, the control power given by (2.9) becomes infinite, as we expect.

(ii) $\psi(p)$ is “positive real” — that is to say:

$\psi(p)$ holomorphic in $\text{Re. } p > 0$

$\psi(p) + \psi(p)^*$ nonsingular, and positive definite, for $\text{Re. } p > 0$

where $*$ denotes conjugate transpose. Of course $\psi(\cdot) \in \mathcal{H}_\infty$.

For the importance of positive realness for robustness, see [6].

Let a compensator transfer function be defined by (2.3) where g and γ are arbitrary, subject only to the condition that

$$\gamma^2 \geq 4g. \quad (3.1)$$

Then for $d_a = 0$ (no actuator noise), the corresponding mean square displacement

$$\lim_{T \rightarrow \infty} \frac{1}{T} \int_0^T \|B^*x(t)\|^2 dt = \frac{d_r g}{2\gamma} \text{Tr. } (B^*A^{-1}B). \quad (3.2)$$

This follows from [1, (6.11)].

4. EXAMPLES: CONTINUUM MODELS

For a given Continuum Model for structures (see [1], [3]) it is possible to reduce (2.3) further to yield finite-dimensional matrix transfer functions which are, however, not rational functions of p . Thus (2.3) becomes:

$$\psi(p) = gpB_u^*(p^2M_b + T(p) + \gamma pB_uB_u^*)^{-1}B_u$$

where

$T(p)$: self-adjoint nonnegative definite nonsingular matrix for $p \geq 0$.
Nonrational meromorphic function of p , $\text{Re. } p > 0$.

B_u is $d \times n$ where

d : number of nodes \times dimension of displacement vector at each node
 n : number of actuators/sensors

M_b is the $d \times d$ mass/moment of inertia matrix corresponding to the nodes. For the SCOLE configuration [1], $d = n = 5$,

$$B_uB_u^* = I_{5 \times 5}$$

and an explicit expression for $T(p)$ is given in [3], and involves hyperbolic sine and cosine functions of p . An example where $d \neq n$ is given by the NASA LaRC Phase Zero Evolutionary Model [4] for which $n = 8$ and $d = 48$. See also [3] for some “textbook” examples for $d = n = 1$, Bernoulli beam bending or torsion.

The system modes are given by

$$M_b p^2 + T(p) = 0. \quad (4.1)$$

5. MODAL APPROXIMATION

Let $\{\phi_k\}$ denote the eigenvectors (mode “shapes”) of the stiffness operator A with ω_k the corresponding eigenvalue (angular frequency). Let b_k denote the corresponding mode “signature” row vector:

$$b_k = (B^* \phi_k)^* \quad 1 \times n \text{ row vector}$$

where n is the number of actuators. Let for each $N \geq 1$,

$$B_N = \begin{bmatrix} b_1 \\ \vdots \\ b_N \end{bmatrix}, \quad D_N = \text{Diagonal}(\omega_1^2, \dots, \omega_N^2).$$

For arbitrary $g, \gamma > 0$, define the compensator transfer function

$$\psi_N(p) = g p B_N^* (p^2 I_N + D_N + \gamma p B_N B_N^*)^{-1} B_N, \quad \text{Re. } p \geq 0. \quad (5.1)$$

Then

- (a) $\psi_N(\cdot)$ is positive real as soon as $B_N^* B_N$ is nonsingular;
- (b) For g, γ defined by (2.4), $\psi_N(p)$ converges to the optimal compensator $\psi(p)$ given by (2.3) as $N \rightarrow \infty$ (and holds *a fortiori* in the finite-dimensional case, where the sequence terminates).

Note that the modal approximation requires only the modes and the “modal signature”: modal displacement at the sensor sites. Note also that (5.1) automatically yields a strictly positive real *rational* transfer function approximation for the case of the Continuum Model — yielding, in fact, a new technique for such approximation. Moreover it has the direct state space representation:

$$\left. \begin{aligned} u(t) &= g B_N^* \dot{Y}(t) \\ \ddot{Y}(t) + D_N \dot{Y}(t) + \gamma B_N B_N^* \dot{Y}(t) &= B_N v(t). \end{aligned} \right\} \quad (5.2)$$

It is also important to note that for a given finite-dimensional modal model with m modes, say, we can choose any N modes for the approximation, not necessarily the first N . Moreover the stability properties of the system are determined by the (“closed-loop”) eigenvalues of the “system” $2(m + N) \times 2(m + N)$ matrix:

$$W = \begin{bmatrix} 0_{m \times m} & I_{m \times m} & 0_{m \times N} & 0_{m \times N} \\ -D_m & 0_{m \times m} & 0_{m \times N} & -g B_m B_m^* \\ 0_{N \times m} & 0_{N \times m} & 0_{N \times N} & I_{N \times N} \\ 0_{N \times m} & B_N B_m^* & -D_N & -\gamma B_N B_N^* \end{bmatrix} \quad (5.3)$$

This is readily seen to be a stable matrix under our condition that $B_N B_N^*$ is nonsingular and $g, \gamma > 0$. Moreover, including a damping matrix $D \geq 0$ in the Truth Model (replace $0_{m \times m}$ in (5.3) by $-D$), we see that

$$\text{Trace } W = -\text{Tr. } D - \gamma \text{Tr. } B_N^* B_N = 2(\text{sum of real parts of eigenvalues}) \quad (5.4)$$

again illustrating the robustness. Also we have

$$\text{product of roots} = |W| = |D_m| \cdot |D_N| \quad (5.5)$$

where $|\cdot|$ denotes determinant. Finally let us note that the eigenvalues are the roots of

$$|pI - W| = |p^2 + D_m + pD| |p^2 + D_N + \gamma p B_N B_N^* + p^2 g B_N B_m^* (p^2 + D_m + pD)^{-1} B_m B_N^*| = 0 \quad (5.6)$$

where the first factor is an $m \times m$ determinant and the second factor is an $N \times N$ determinant, if $g = 0$ structure modes are unaffected. We can see from (5.4) - (5.6) that the total damping increases as γ is increased but the damping in the structure modes can decrease depending on how large γ is. Thus, for each fixed value of the gain g , there is apparently an optimal choice for γ , which may depend on the mode frequency in general.

6. SIMULATION RESULTS: PHASE ZERO EVOLUTIONARY MODEL, NASA LaRC

For evaluating control performance by simulation, the NASA LaRC CSI Phase-Zero Evolutionary model data [4] is used — specifically, the modes and modal signatures.

We denote by m the number of modes in the truth model of the structure, and let N = the number of modes in the compensator, as in (5.2) and (5.3). The compensator is thus characterized by the “gain” parameter g , the “damping” parameter γ , and N the number of “control” modes (or $2N$ = number of states). Note that for each N

$$\Psi_N(p) \rightarrow kI \quad (\sim \text{“direct connection” or “static controller”})$$

as $g \rightarrow \infty, \gamma \rightarrow \infty$, keeping the ratio

$$\frac{g}{\gamma} = k \quad (6.1)$$

fixed. Also for $N = m$, we can use (3.2) to determine the mean square displacement where now

$$\text{Tr. } B^* A^{-1} B = \sum_1^m \frac{\|b_k\|^2}{\omega_k^2},$$

so that the mean square displacement can be expressed

$$= \frac{d_r g}{2\gamma} \sum_1^m \frac{\|b_k\|^2}{\omega_k^2}, \quad \gamma^2 > 4g, \quad (6.2)$$

and thus increases with g and decreases as γ increases.

Data for the modal model of the NASA LaRC Phase Zero Evolutionary Model is taken from [4]. Here $n = 8$ so that each b_k is 8×1 , and m for the Truth model is 86, and $D = 0$ (no damping). In this case the optimal compensator will use all 86 modes. Table I[§] shows the mode frequencies and a typical mode shape (b_7). B^*B_8 is nonsingular.

Figures 1, 2, and 3 show the behavior of the damping ratio for fixed g as a function of the damping parameter γ , for angular frequencies 314 (the 86th mode), 106 (the 43rd mode) and 9.25 (the 7th mode), respectively. Note the occurrence of the maximum for all around $\gamma = 8$. Figures 4, 5, and 6 show the attainable damping ratios for a compensator with $N = 30$, and the same gain

§ Personal communication, S. M. Joshi, NASA LaRC, 1992.

Mode Number	(Angular) Frequency rad/sec	Mode Number	(Angular) Frequency rad/sec	Mode Number	(Angular) Frequency rad/sec	Mode Number	(Angular) Frequency rad/sec
1 =	0.9243	23 =	38.8269	45 =	120.5899	67 =	195.1799
2 =	0.9365	24 =	39.1489	46 =	133.1399	68 =	196.9100
3 =	0.9752	25 =	40.6580	47 =	137.8399	69 =	198.1300
4 =	4.5872	26 =	41.9080	48 =	139.5700	70 =	198.7400
5 =	4.6985	27 =	46.3219	49 =	147.2599	71 =	203.3300
6 =	5.4913	28 =	52.1080	50 =	154.2500	72 =	209.7299
7 =	9.2580	29 =	52.8380	51 =	156.5399	73 =	231.7400
8 =	10.9209	30 =	53.1319	52 =	156.9199	74 =	232.9499
9 =	11.8310	31 =	55.4410	53 =	161.0299	75 =	239.8899
10 =	14.4600	32 =	56.0859	54 =	164.6499	76 =	241.4499
11 =	15.9259	33 =	56.3370	55 =	165.1399	77 =	244.9299
12 =	17.8349	34 =	58.0239	56 =	166.9100	78 =	244.9900
13 =	21.4850	35 =	59.8600	57 =	170.8300	79 =	247.8300
14 =	21.9050	36 =	62.2190	58 =	173.7700	80 =	255.7700
15 =	22.5400	37 =	78.4509	59 =	180.0099	81 =	268.6499
16 =	25.2250	38 =	85.5439	60 =	181.9100	82 =	270.5499
17 =	25.3349	39 =	89.9440	61 =	183.1300	83 =	275.7200
18 =	26.4249	40 =	92.4779	62 =	186.6199	84 =	287.5299
19 =	27.5949	41 =	99.8170	63 =	187.7500	85 =	308.7500
20 =	31.6009	42 =	105.8899	64 =	191.2400	86 =	314.2399
21 =	31.6289	43 =	106.7699	65 =	192.0599		
22 =	34.5660	44 =	116.1500	66 =	193.7899		

Mode Shape b_7

-0.9084100127220	-0.0009229300194	0.4756200015545	0.0040255999193
0.0009075700073	-0.4345000088215	-0.0070441002026	1.1181999444962

Table I. Mode Frequencies And Sample Mode Shape

$g (= 20)$, but here there is no maximum for the mode frequency of 314 which is not included in the controller modes. For the mode frequencies 9 and 106, the maximum occurs around $\gamma = 5$ and $\gamma = 30$, respectively. Table II shows the damping ratios for all (angular) frequencies (both control and structure modes; the former have higher damping) between 1 and 150 for $g = 20$ and $\gamma = 5$ for the optimal compensator ($N = 86$). Table III shows the same for $N = 30$. The damping ratios are seen to compare favorably with those reported in [5, 6], depending of course on the appropriate gain setting, but detailed comparative evaluation will need further study. Table IV shows the damping ratios for zero gain ($g = 0$) with $N = 86$ and $\gamma = 10$ which should help distinguish the control modes from structure modes (the latter have zero damping). Figure 7 shows the damping ratio as a function of g for $N = 86$, $\gamma = 10$ and mode frequency 21.485. The damping increases for the structure mode and decreases for the control mode.

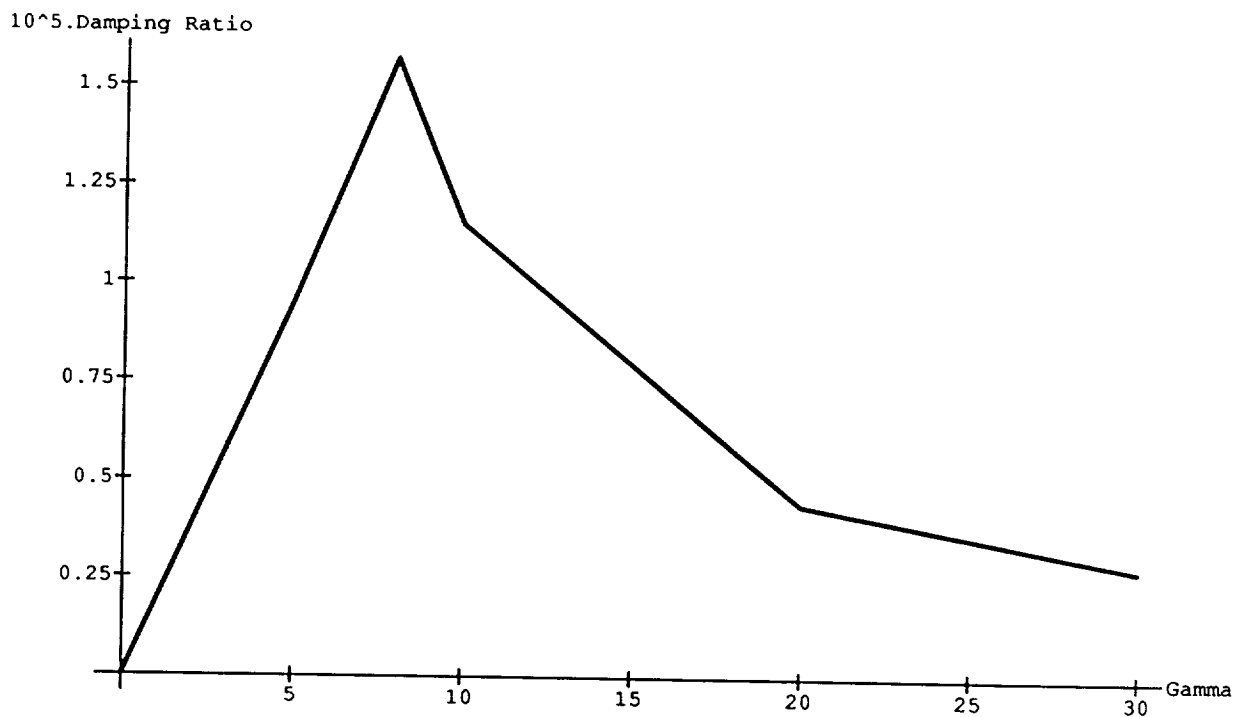


Figure 1. Damping ratio vs. damping parameter γ : mode angular frequency 314; $N = 86$.

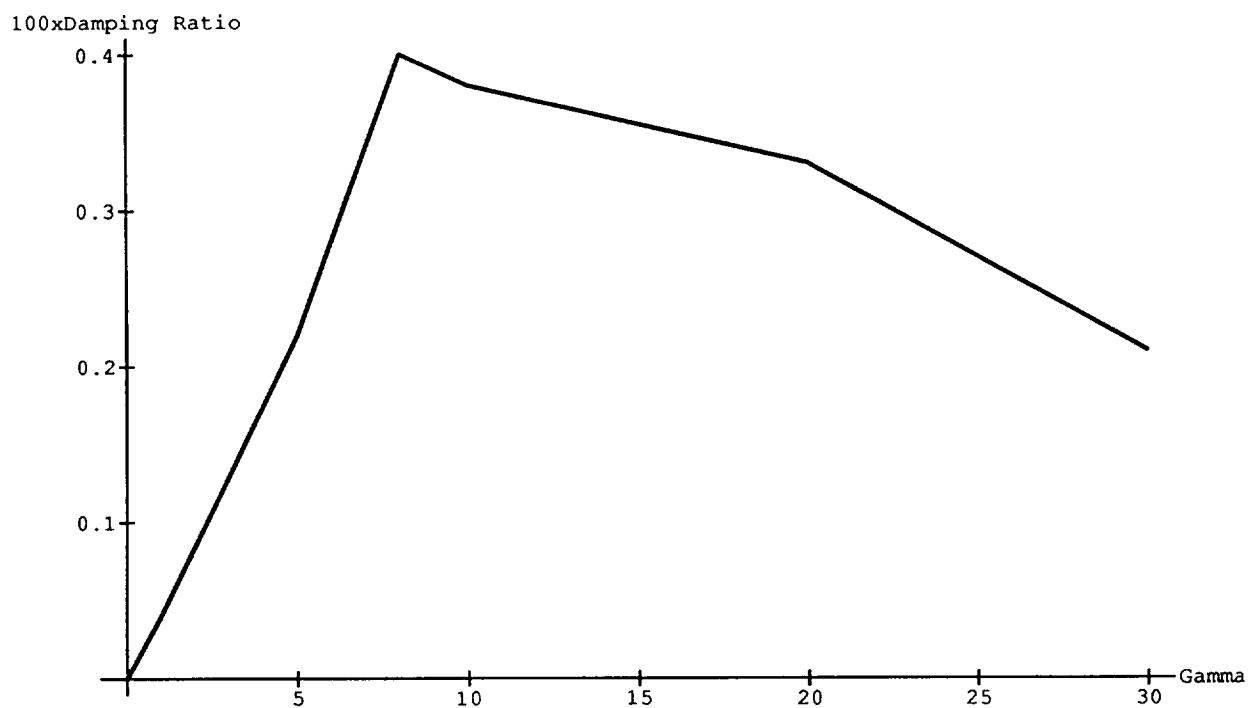


Figure 2. Damping ratio vs. damping parameter γ : mode angular frequency 106; $N = 86$.

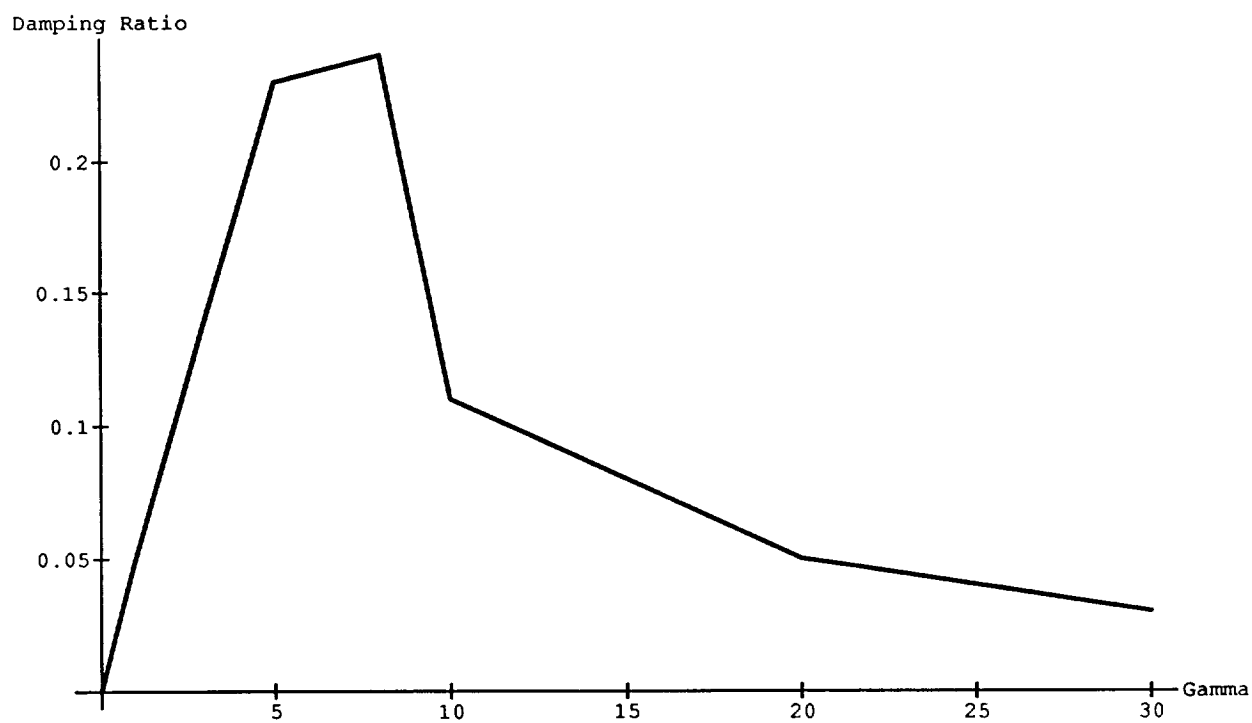


Figure 3. Damping ratio vs. damping parameter γ : mode angular frequency 9.25; $N = 86$.

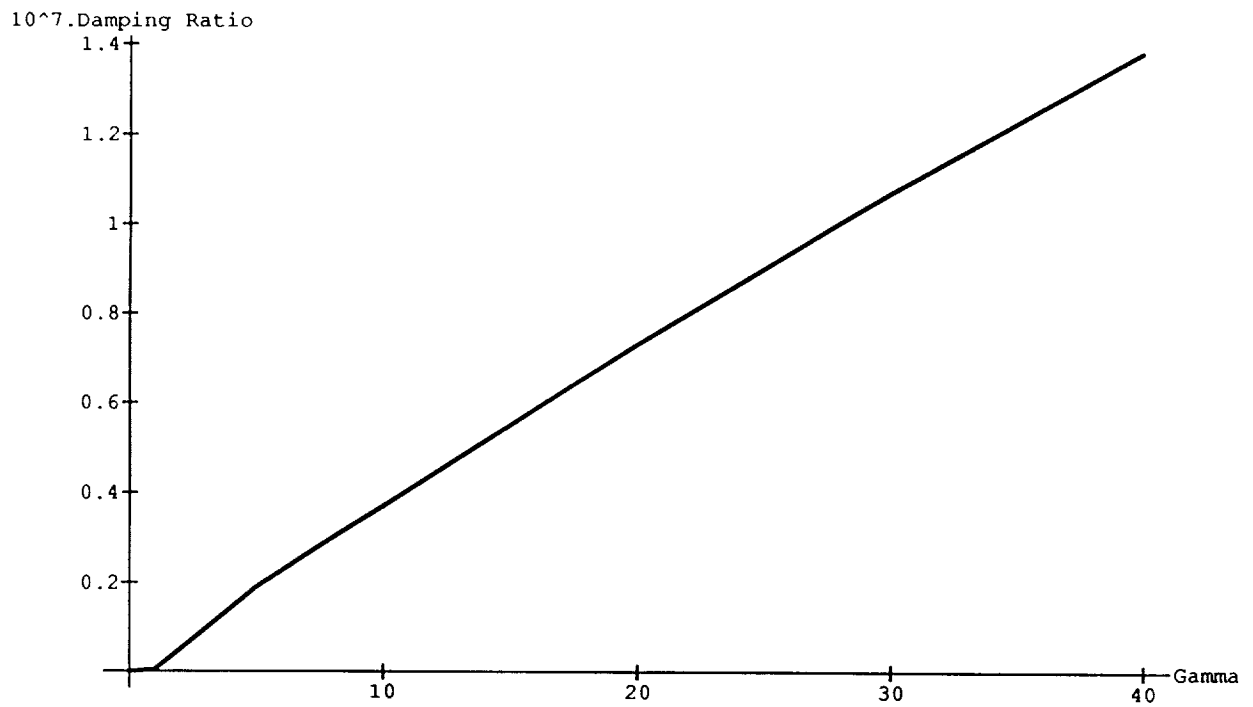


Figure 4. Damping ratio vs. damping parameter γ : mode angular frequency 314; $N = 30$.

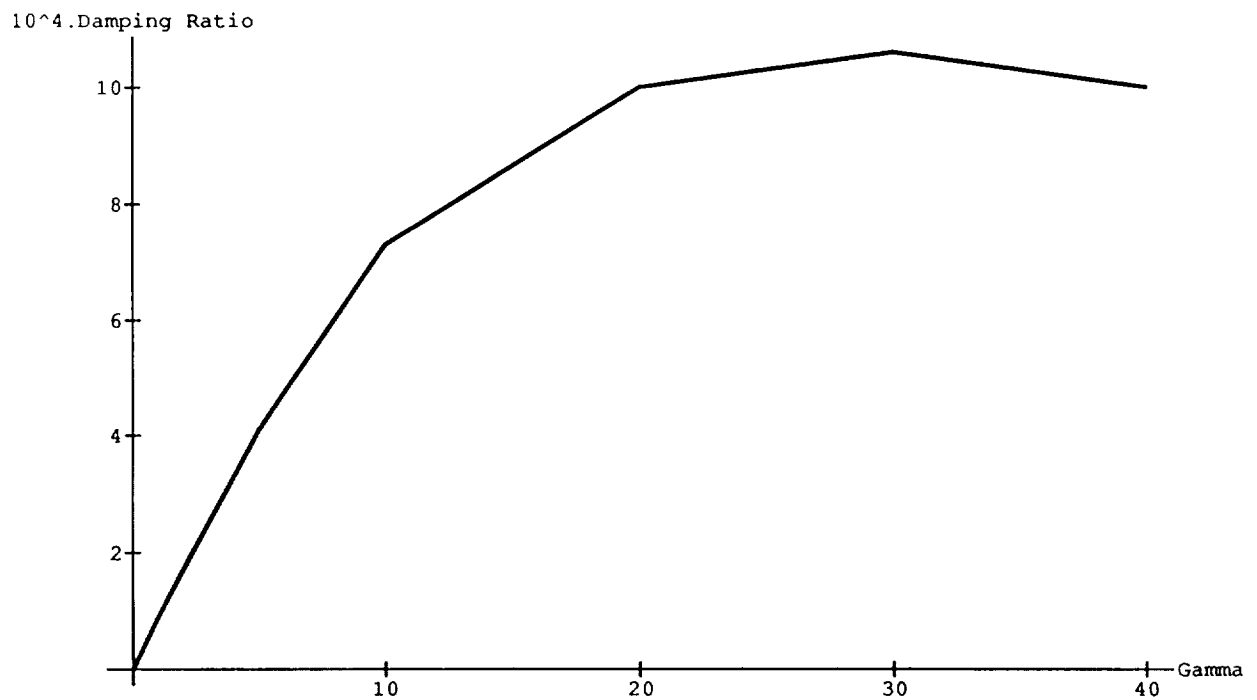


Figure 5. Damping ratio vs. damping parameter γ : mode angular frequency 106; $N = 30$.

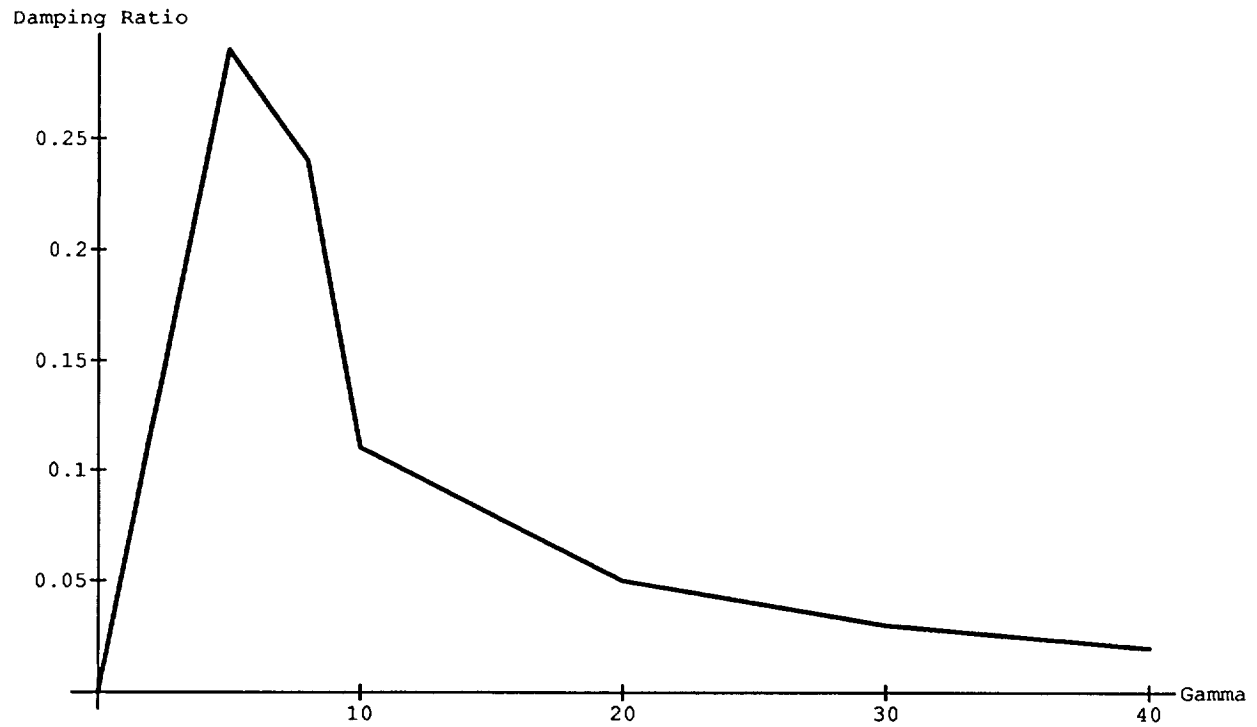


Figure 6. Damping ratio vs. damping parameter γ : mode angular frequency 9.25; $N = 30$.

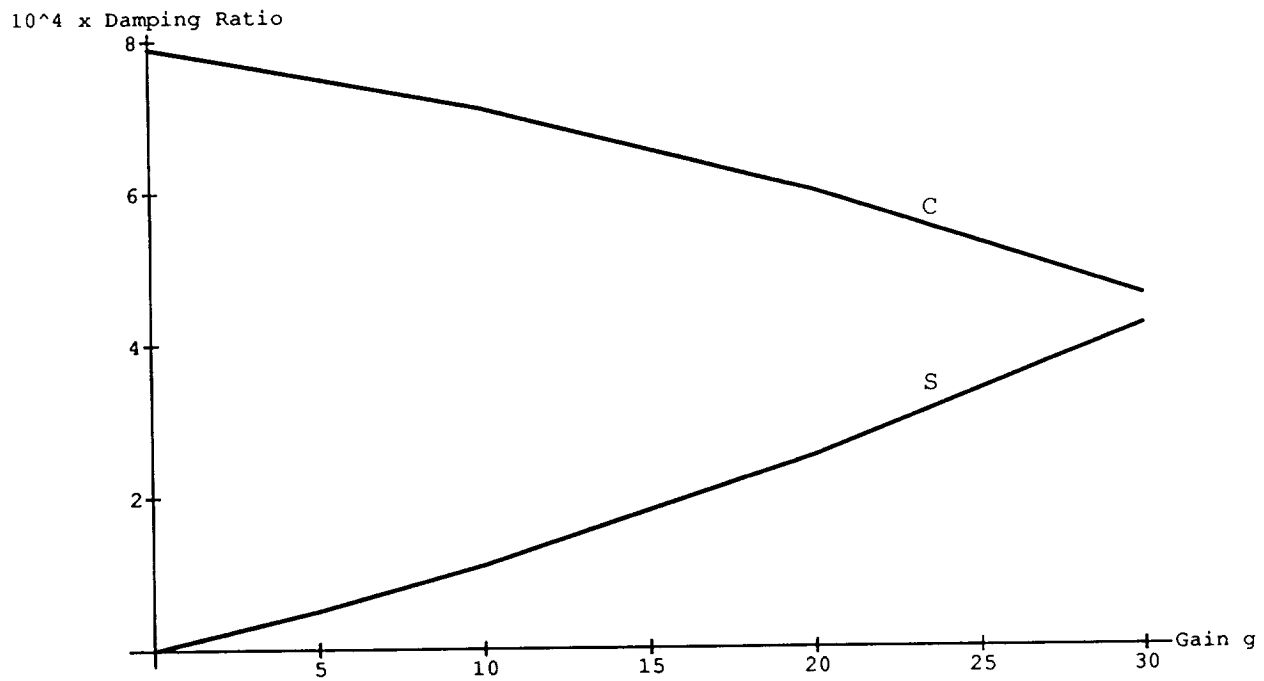


Figure 7. Damping ratio vs. g : mode frequency 21.49 r/s; $N = 86$; $\gamma = 10$; C: control; S: structure

Angular Frequency	Damping Ratio	Angular Frequency	Damping Ratio	Angular Frequency	Damping Ratio
.17106E+01	.48814E+00	.27975E+02	.10362E+00	.61950E+02	.10323E+00
.25233E+01	.42349E+00	.30735E+02	.22514E+00	.62123E+02	.77622E-03
.38285E+01	.18903E+00	.30903E+02	.16990E+00	.62301E+02	.15341E-02
.40291E+01	.53048E+00	.31554E+02	.10862E-02	.77219E+02	.89300E-02
.50981E+01	.53701E-01	.31573E+02	.34084E-02	.79869E+02	.16028E-01
.55010E+01	.27800E+00	.31601E+02	.36615E-05	.85536E+02	.45737E-04
.62846E+01	.48991E+00	.31601E+02	.60475E-05	.85554E+02	.13440E-03
.65389E+01	.15363E+00	.33265E+02	.29600E-01	.89610E+02	.18167E-02
.73598E+01	.25791E+00	.35339E+02	.12758E-01	.90357E+02	.56712E-02
.88473E+01	.28576E+00	.36245E+02	.22248E-01	.92127E+02	.21810E-02
.96096E+01	.23182E+00	.38097E+02	.15841E-01	.92875E+02	.35775E-02
.98633E+01	.46814E-01	.39485E+02	.23587E-01	.99737E+02	.42099E-03
.14333E+02	.26440E-02	.39715E+02	.64462E-02	.99912E+02	.10766E-02
.14370E+02	.13551E-01	.40253E+02	.96291E-02	.10474E+03	.62417E-02
.15912E+02	.94853E-03	.42723E+02	.40264E-01	.10629E+03	.21788E-02
.15918E+02	.12789E-03	.47595E+02	.20357E+00	.10703E+03	.53890E-02
.16858E+02	.34110E+00	.49116E+02	.37251E-01	.10757E+03	.10741E-01
.17438E+02	.15497E-01	.50628E+02	.74785E-01	.11586E+03	.14946E-02
.17615E+02	.36468E-02	.52567E+02	.48805E-03	.11648E+03	.24414E-02
.18676E+02	.27518E+00	.52612E+02	.36127E-03	.12059E+03	.22062E-04
.21478E+02	.26988E-03	.52923E+02	.23978E-01	.12059E+03	.32178E-04
.21491E+02	.25982E-03	.53030E+02	.65234E-03	.13306E+03	.38080E-03
.21897E+02	.29663E-03	.53116E+02	.39229E-02	.13322E+03	.42566E-03
.21913E+02	.24238E-03	.55388E+02	.51163E-03	.13759E+03	.12103E-02
.22536E+02	.20344E-03	.55476E+02	.11573E-02	.13809E+03	.12406E-02
.22544E+02	.20967E-03	.55627E+02	.47474E-01	.13957E+03	.39718E-05
.23354E+02	.22881E+00	.55777E+02	.20228E+00	.13957E+03	.50153E-05
.23666E+02	.31516E-01	.56012E+02	.50958E-03	.14684E+03	.17338E-02
.25234E+02	.10998E-02	.56120E+02	.32213E-02	.14771E+03	.22478E-02
.25241E+02	.24057E-03	.57973E+02	.33939E-03		
.25492E+02	.34385E-01	.58058E+02	.22112E-02		
.26321E+02	.16274E-02	.59857E+02	.16844E-04		
.26361E+02	.82509E-03	.59860E+02	.10358E-03		

Table II. Damping Ratio Vs. Angular Frequency: $N = 86$; $g = 20$; $\gamma = 5$

Angular Frequency	Damping Ratio	Angular Frequency	Damping Ratio	Angular Frequency	Damping Ratio
.17111E+01	.48787E+00	.27681E+02	.10975E+00	.92550E+02	.19914E-03
.25240E+01	.42289E+00	.30664E+02	.22748E+00	.99846E+02	.13752E-03
.38283E+01	.18850E+00	.30908E+02	.16861E+00	.10612E+03	.41269E-03
.40268E+01	.53155E+00	.31554E+02	.10567E-02	.10689E+03	.23571E-03
.50982E+01	.53764E-01	.31573E+02	.34060E-02	.11618E+03	.42708E-04
.55074E+01	.27646E+00	.31601E+02	.36214E-05	.12059E+03	.81852E-06
.62704E+01	.49202E+00	.31601E+02	.60906E-05	.13315E+03	.42638E-05
.65413E+01	.15327E+00	.33268E+02	.29376E-01	.13785E+03	.64145E-05
.73966E+01	.25589E+00	.35300E+02	.13261E-01	.13957E+03	.88491E-07
.88395E+01	.28765E+00	.36246E+02	.21919E-01	.14728E+03	.89389E-05
.96114E+01	.24204E+00	.38090E+02	.15162E-01		
.98657E+01	.46669E-01	.39472E+02	.24008E-01		
.14333E+02	.26268E-02	.39716E+02	.61748E-02		
.14371E+02	.13622E-01	.40247E+02	.98628E-02		
.15912E+02	.94628E-03	.42747E+02	.38763E-01		
.15918E+02	.12646E-03	.47582E+02	.20393E+00		
.16873E+02	.34829E+00	.49299E+02	.30838E-01		
.17439E+02	.15483E-01	.50456E+02	.78217E-01		
.17615E+02	.36319E-02	.52567E+02	.50746E-03		
.18473E+02	.29242E+00	.52615E+02	.32023E-03		
.21478E+02	.26755E-03	.53031E+02	.60754E-03		
.21491E+02	.26123E-03	.53108E+02	.36922E-02		
.21897E+02	.29369E-03	.55446E+02	.30132E-03		
.21913E+02	.24459E-03	.55694E+02	.20493E+00		
.22536E+02	.19617E-03	.55773E+02	.44503E-01		
.22544E+02	.21245E-03	.56112E+02	.13185E-02		
.23367E+02	.23050E+00	.58052E+02	.72573E-03		
.23680E+02	.29890E-01	.58417E+02	.24337E-01		
.25234E+02	.11092E-02	.59861E+02	.78116E-04		
.25241E+02	.24125E-03	.62235E+02	.19700E-03		
.25495E+02	.33946E-01	.78798E+02	.19928E-02		
.26323E+02	.16797E-02	.85547E+02	.18896E-04		
.26362E+02	.80854E-03	.90088E+02	.74096E-03		

Table III. Damping Ratio vs. Angular Frequency: $N = 30$; $g = 20$; $\gamma = 5$

Angular Frequency	Damping Ratio	Angular Frequency	Damping Ratio	Angular Frequency	Damping Ratio
.45872E+01	.00000E+00	.31629E+02	.00000E+00	.89479E+02	.73662E-02
.46986E+01	.00000E+00	.34566E+02	.00000E+00	.89944E+02	.00000E+00
.53549E+01	.10629E+00	.35259E+02	.24327E-01	.92185E+02	.99239E-02
.54914E+01	.00000E+00	.38762E+02	.32907E-01	.92478E+02	.00000E+00
.89044E+01	.84249E-01	.38827E+02	.00000E+00	.99727E+02	.17443E-02
.92581E+01	.00000E+00	.39149E+02	.00000E+00	.99817E+02	.00000E+00
.10921E+02	.00000E+00	.39744E+02	.22024E-01	.10466E+03	.29513E-01
.11831E+02	.00000E+00	.40658E+02	.00000E+00	.10589E+03	.00000E+00
.13632E+02	.17079E+01	.41118E+02	.24327E+00	.10616E+03	.92339E-02
.14263E+02	.77629E-02	.41908E+02	.00000E+00	.10677E+03	.00000E+00
.14460E+02	.00000E+00	.46322E+02	.00000E+00	.11595E+03	.63634E-02
.15914E+02	.28005E-03	.46630E+02	.20336E+00	.11615E+03	.00000E+00
.15926E+02	.00000E+00	.50739E+02	.80977E-01	.12059E+03	.97457E-04
.17552E+02	.82357E-02	.52108E+02	.00000E+00	.12059E+03	.00000E+00
.17835E+02	.00000E+00	.52588E+02	.42582E-03	.13312E+03	.15997E-02
.21485E+02	.00000E+00	.52838E+02	.00000E+00	.13314E+03	.00000E+00
.21487E+02	.78458E-03	.52988E+02	.21608E-02	.13783E+03	.49739E-02
.21905E+02	.00000E+00	.53132E+02	.00000E+00	.13784E+03	.00000E+00
.21907E+02	.90374E-03	.55387E+02	.22200E-02	.13957E+03	.16752E-04
.22375E+02	.13007E+00	.55441E+02	.00000E+00	.13957E+03	.00000E+00
.22540E+02	.00000E+00	.55964E+02	.17243E-02	.14705E+03	.77790E-02
.22541E+02	.24691E-03	.56086E+02	.00000E+00	.14726E+03	.00000E+00
.24459E+02	.13332E+00	.56337E+02	.00000E+00		
.25225E+02	.00000E+00	.57938E+02	.11515E-02		
.25243E+02	.45734E-03	.58024E+02	.00000E+00		
.25335E+02	.00000E+00	.59855E+02	.51996E-04		
.26335E+02	.13181E-02	.59860E+02	.00000E+00		
.26425E+02	.00000E+00	.62125E+02	.34738E-02		
.27595E+02	.00000E+00	.62211E+02	.00000E+00		
.30456E+02	.13725E+00	.77305E+02	.39799E-01		
.31563E+02	.30544E-02	.78451E+02	.00000E+00		
.31601E+02	.00000E+00	.85533E+02	.19002E-03		
.31601E+02	.11152E-04	.85544E+02	.00000E+00		

Table IV. Damping: Zero Gain: $N = 86$; $\gamma = 10$

7. CONCLUSIONS

A class of compensators in explicit form (not requiring computer calculations) has been presented for stabilizing flexibility structures with collocated rate sensors. They are optimized for the LQG criterion for minimizing the mean square rate and hence have inherently good noise response features. They are robust with respect to system stability, can be instrumented in state space form suitable for digital control and above all can be specified to any complexity desired directly from the structure modes and mode signatures at the sensor sites. Simulation results are presented for the modal model of the NASA LaRC Phase Zero Evolutionary Model — mainly damping ratios attainable and their dependence on compensator design parameters and complexity. The damping ratios compare favorably with those reported in [5, 6], but any detailed comparative evaluation of course is possible only after further study.

REFERENCES

1. Balakrishnan, A. V.: Compensator Design for Stability Enhancement with Collocated Controllers," *IEEE Transactions on Automatic Control*, vol. 36, no. 9, September 1991, pp. 994-1007.
2. Balakrishnan, A. V.: Modes of Interconnected Lattice Trusses Using Continuum Models, Part 1, NASA CR 189568, December 1991.

3. Balakrishnan, A. V.: Compensator Design for Stability Enhancement with Collocated Controllers: Explicit Solutions. *IEEE Transactions on Automatic Control*, vol. 37, no. 1, January 1993.
4. Belvin, W. K.; Horta, L. G.; and Elliott, K. E.: The LaRC CSI Phase-0 Evolutionary Model Test Bed: Design and Experimental Results. Paper presented at the 4th Annual NASA-DOD Conference on CSI Technology, November 5-7, 1990, Orlando, Florida.
5. Lim, K. B.; Maghami, P. G.; and Joshi, S. M.: A comparison of controller designs for an experimental flexible structure. Paper presented at the 1991 American Control Conference, June 1991, Boston, Massachusetts.
6. Joshi, S. M.; Maghami, P. G.; and Kelkar, A. G.: Dynamic Dissipative Compensator Design for Large Space Structures." AIAA-91-2650, August 1991.